

Supplementary Materials for

Overcoming resistance to EGFR monotherapy in HNSCC by identification and inhibition of individualized cancer processes

Maria R. Jubran¹, Daniela Vilenski¹, Efrat Flashner-Abramson¹, Efraim Shnaider¹, Swetha Vasudevan¹, Ariel M. Rubinstein¹, Amichay Meirovitz², Shay Sharon³, David Polak^{4*} and Nataly Kravchenko-Balasha^{1*}

¹The Institute of Biomedical and Oral Research, Hebrew University of Jerusalem, Jerusalem 91120, Israel

² Sharett Institute of Oncology, Hebrew University-Hadassah Medical Center, Jerusalem, Israel.

³ Department of Oral and Maxillofacial Surgery, The Hebrew University and Hadassah Medical Center, Jerusalem, Israel.

⁴ Department of Periodontics, Faculty of Dental Medicine, The Hebrew University and Hadassah Medical Center, Jerusalem, Israel.

*Corresponding authors: natalyk@ekmd.huji.ac.il, polak@mail.huji.ac.il

This PDF file includes:

- 1. Figures S1 to S5**
- 2. Supplementary References**

Figure S1

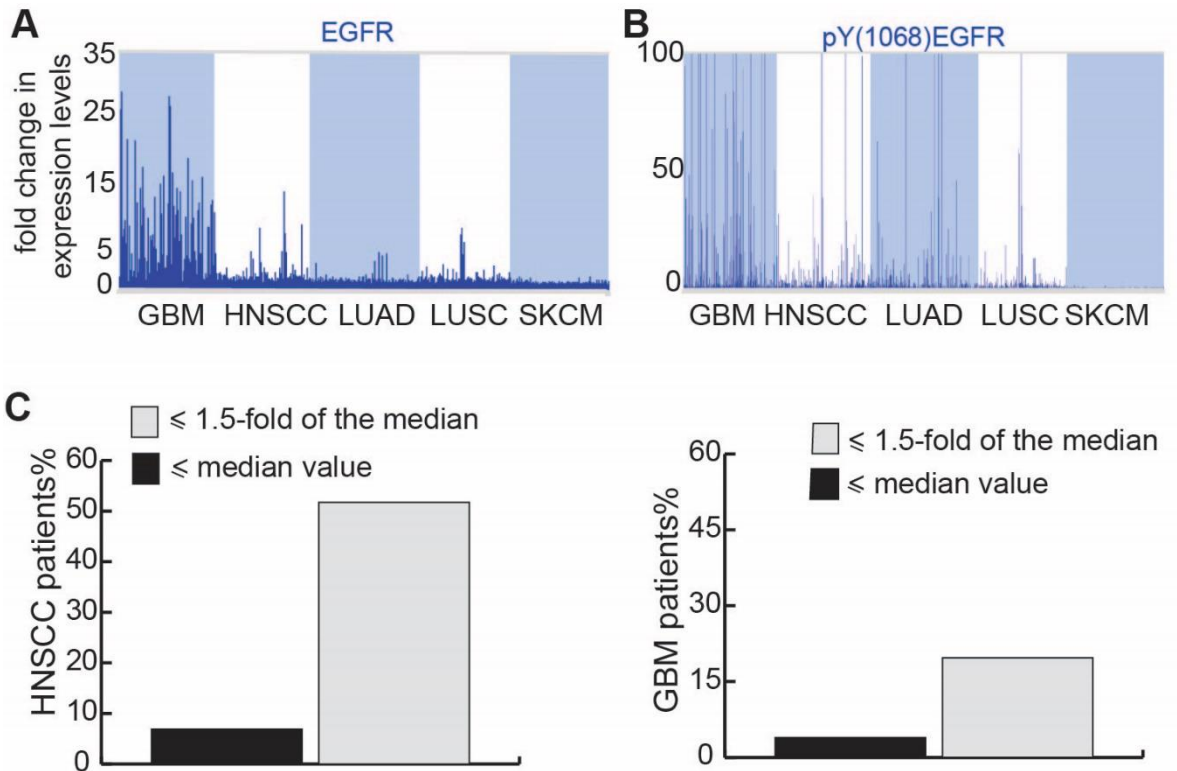
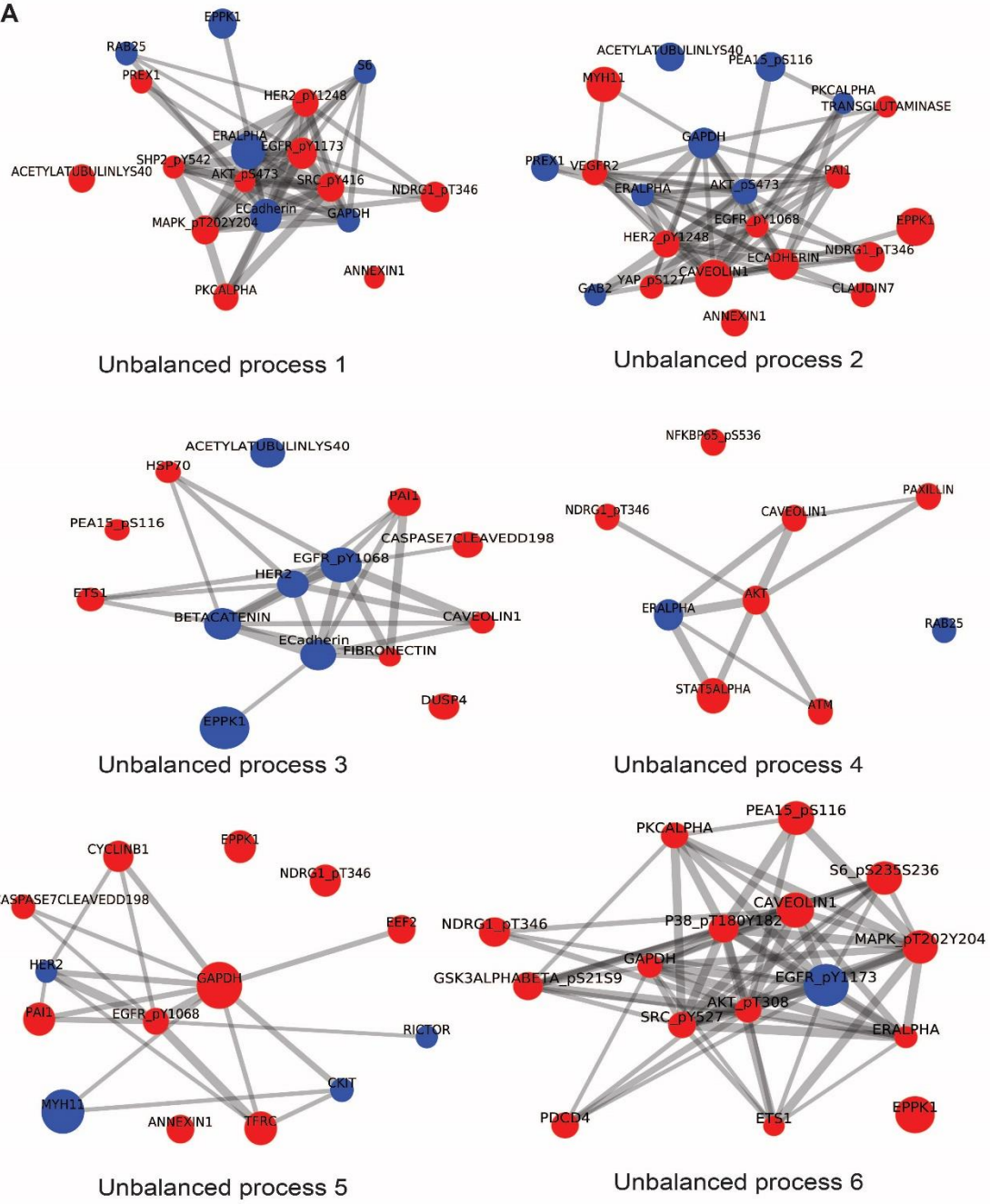
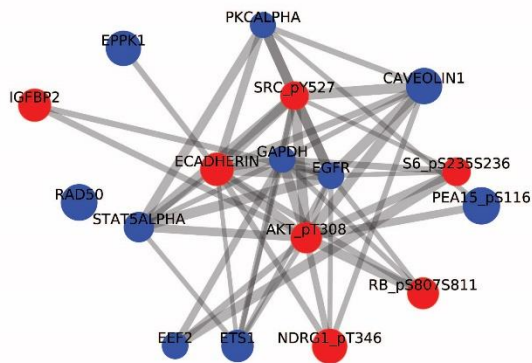


Figure S1. Variability in EGFR expression levels in different cancer types. EGFR expression pattern in 5 tumor types is presented. EGFR protein (A) and EGFR phospho-protein expression levels (B) are compared between GBM, HNSCC, LUAD, LUSC and SKCM cancer types and within each type. (C) Percentage of HNSCC and GBM patients that harbor relatively low EGFR levels in comparison with the median values in the dataset.

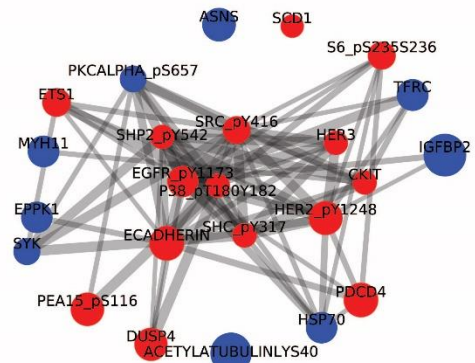
Figure S2

A

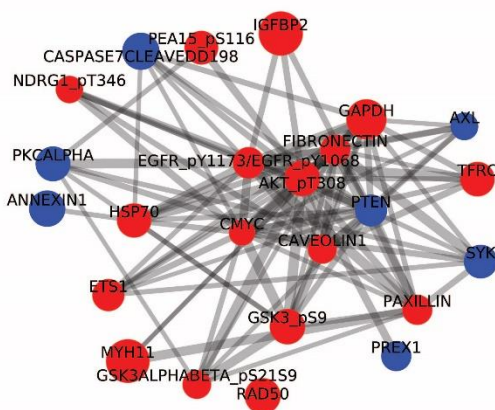




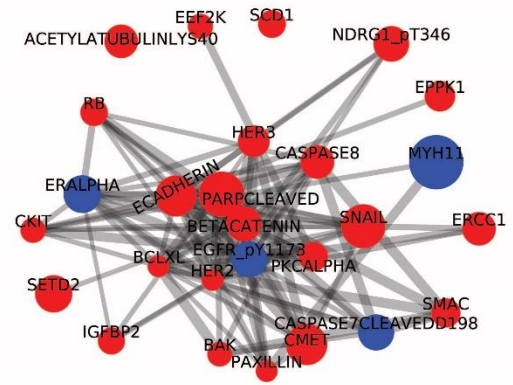
Unbalanced process 7



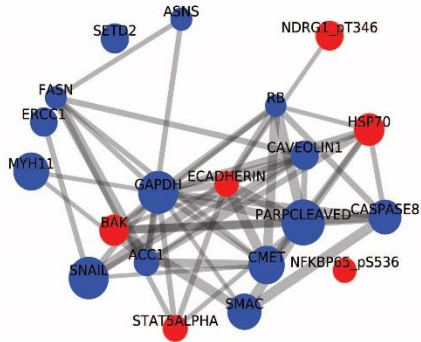
Unbalanced process 8



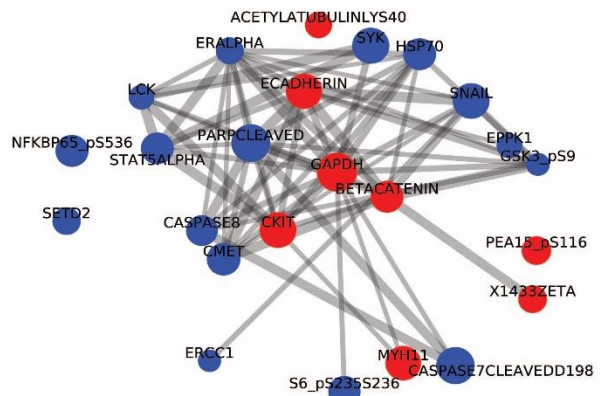
Unbalanced process 9



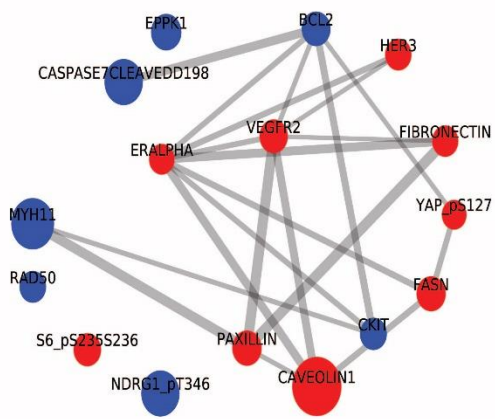
Unbalanced process 10



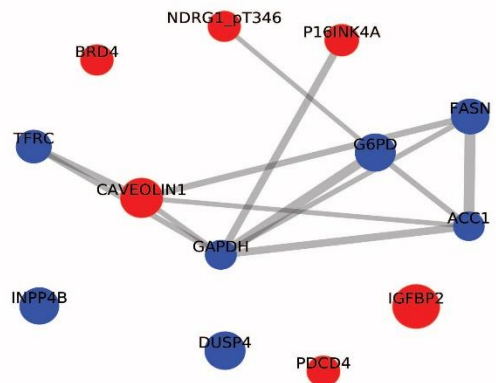
Unbalanced process 11



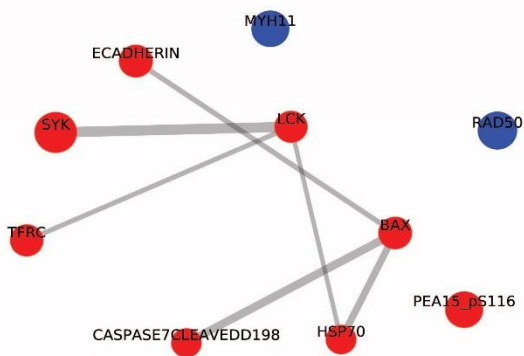
Unbalanced process 12



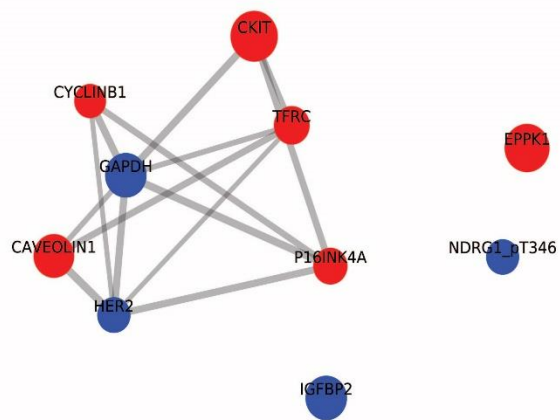
Unbalanced process 13



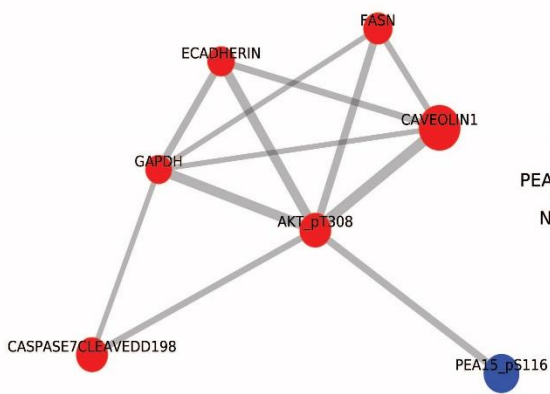
Unbalanced process 14



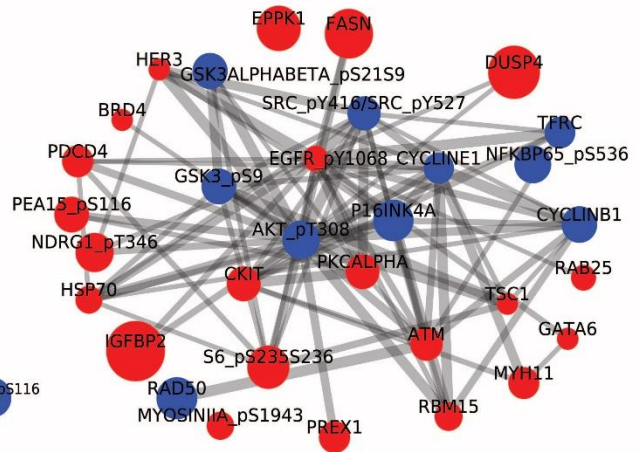
Unbalanced process 15



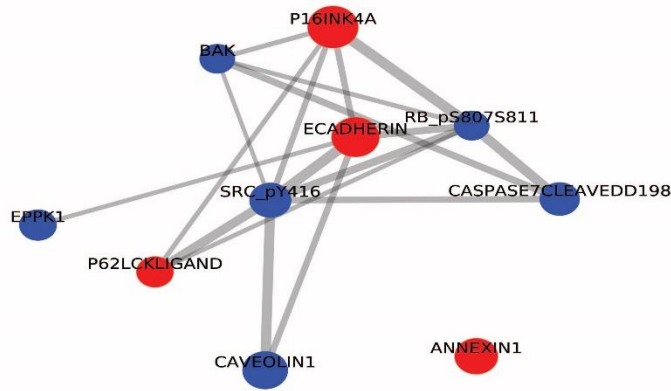
Unbalanced process 16



Unbalanced process 17



Unbalanced process 18



Unbalanced process 19

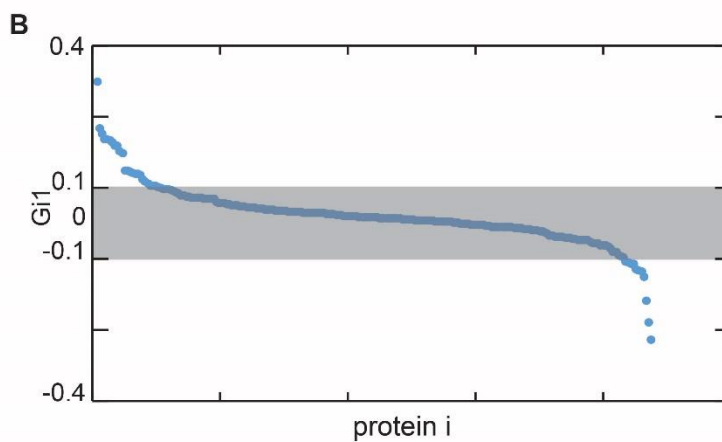


Figure S2. 19 unbalanced subnetworks, as identified by surprisal analysis, found to be active in 1038 tumors. (A) 19 unbalanced processes (subnetworks) characterizing 1038 patients are shown. See Figure S3 demonstrating how the number of processes was determined. Proteins with negative $G_{i\alpha}$ values are labeled in blue and proteins with positive $G_{i\alpha}$ values in red, to distinguish between *correlated* and *anti-correlated* proteins. Circle sizes, denoting participating proteins in the process, are defined by $G_{i\alpha}$ values. The procedure calculating induction or reduction in expression levels includes calculation of the product, $G_{i\alpha}\lambda_{\alpha}(k)$, which denotes a deviation in expression levels from the reference state due to process α . Positive values of $G_{i\alpha}\lambda_{\alpha}(k)$ mean induction relative to the steady state, and negative values mean reduction. For more details see references [1–3]. (B) Proteins must have a significant $G_{i\alpha}$ (which represent the degree of participation of every protein i in the unbalanced process α , see Methods for more details) values to be included in the unbalanced process α . The proteins that take part in the different unbalanced processes were identified as follows: for every unbalanced process α , $G_{i\alpha}$ values were sorted according to their size, and only proteins (i) with significant $G_{i\alpha}$ values were considered to participate in the unbalanced process α . This is exemplified for the process $\alpha = 1$. In the figure sorted values of G_{i1} are shown. The gray box represents threshold values. Proteins with $G_{i1} > 0.1$ or $G_{i1} < -0.1$ (which form the top and bottom "tails" of the distribution) were considered to participate the most in the unbalanced process $\alpha = 1$. These proteins were used to build a functional subnetwork using STRING database (showed in A).

Figure S3

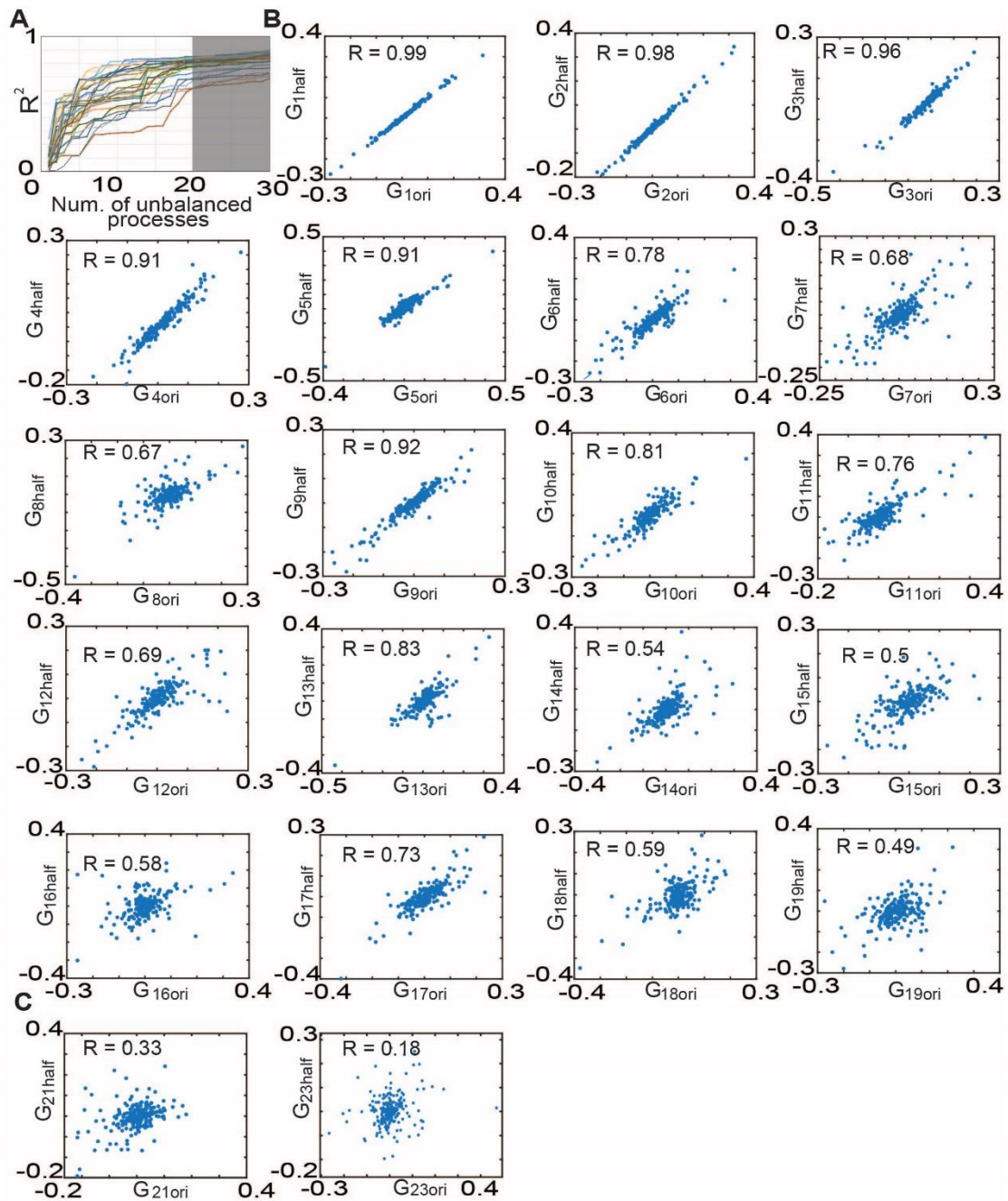
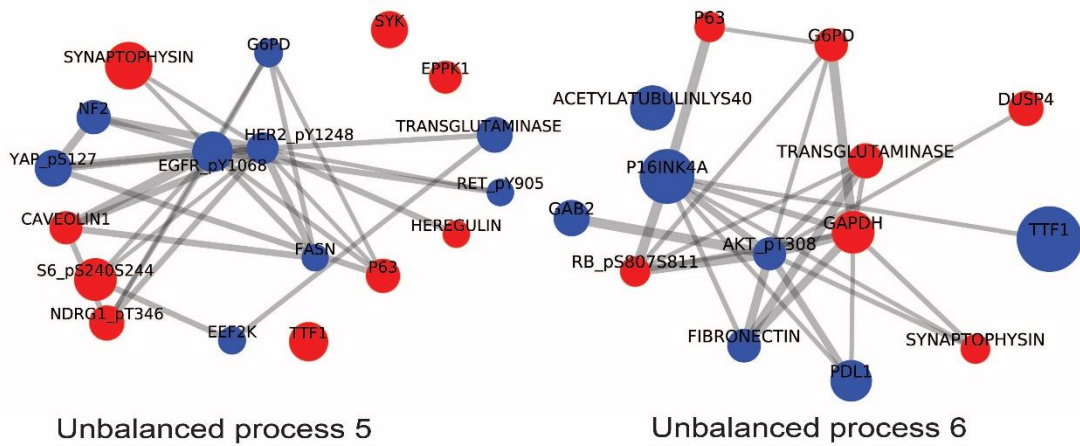
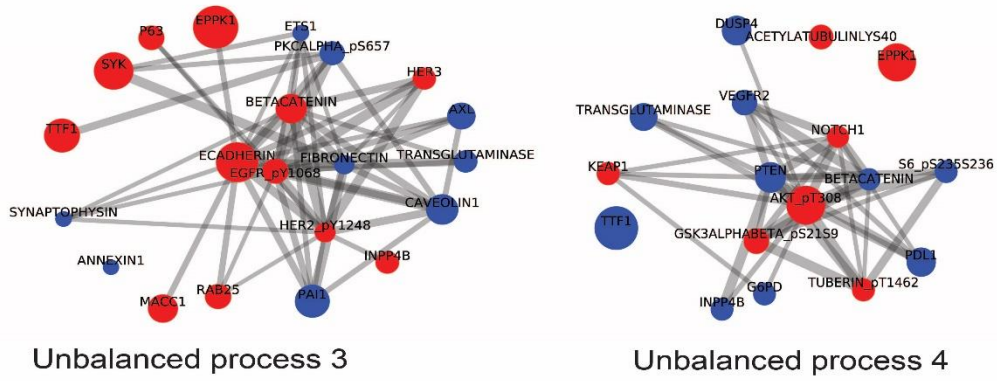
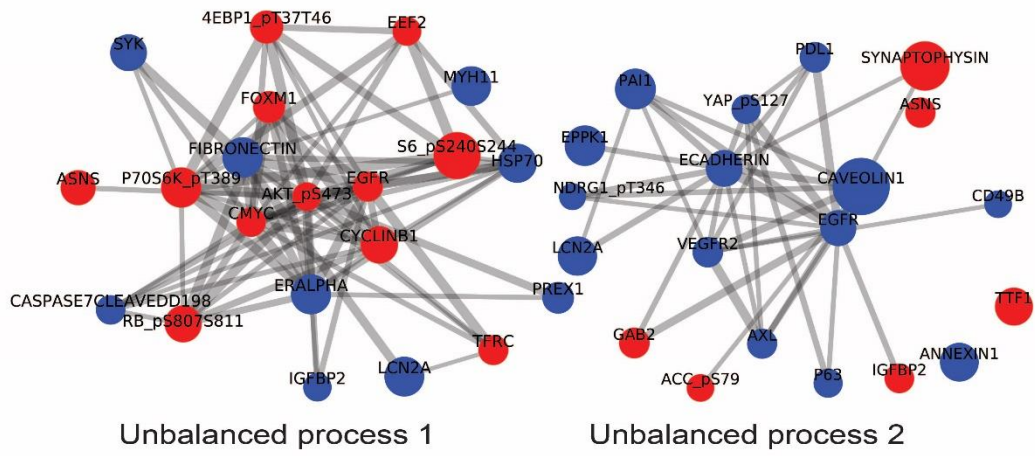


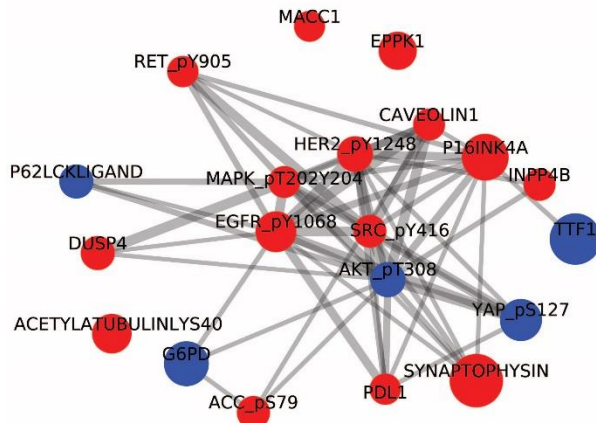
Figure S3. 19 unbalanced processes reproduce the experimental data. (A) R^2 values, reflecting the correlation between the experimental expression data and the theoretical calculations, were calculated in order to determine how many processes are required in order to reproduce the experimental data. As we add more unbalanced processes we expect to get higher correlation between the experimental data and the theoretical calculation, reaching the highest level of correlation when the experimental data is reproduced by the theoretical fitting. When the R^2 values reach a plateau, that means that we do not add real processes, but mainly noise. Correlation plots between theoretical calculations and the experimental data are shown for 30 selected patients, harboring different types of cancer. R^2 was calculated by plotting the natural logarithm of the experimental data ($\text{Ln}X_i$) vs $\sum G_{i\alpha}\lambda_{\alpha}(k)$ for $\alpha = 1-30$ (denoted as

Num. of unbalanced processes in the plot). $G_{i\alpha}$ denotes weight of protein i in a process α . $\lambda_{\alpha}(k)$ denotes amplitude of a process α in each patient k . Product, $G_{i\alpha}\lambda_{\alpha}(k)$, denotes a deviation in expression levels from the reference state due to process α . $\sum G_{i\alpha}\lambda_{\alpha}(k)$ is the sum of all the processes in which each protein participates (For more details see [1–3]). The plot reaches a plateau after the 19th process. This indicates that after the 19th process the data includes mainly noise. **(B)** Unbalanced processes remained the same when either the entire dataset or a subset of the dataset are used for the analysis. The weights of the proteins in the significant unbalanced processes ($\alpha = 1-19$) were found to be similar when either the entire dataset (original (ori) dataset, 1038 patients) or only half the population of patients from each dataset (521 patients) were analyzed as indicated by the high correlation of the scatter plots. The correlation coefficient R is above 0.9 for the processes 0,1,2,3,4,5,and 9 and is above 0.65 for the processes 6,7,8,10,11,12,13 and 17. **(C)** The correlation coefficient R was significantly lower when the unbalanced processes 21, 23 were compared indicating that those processes represent mainly noise.

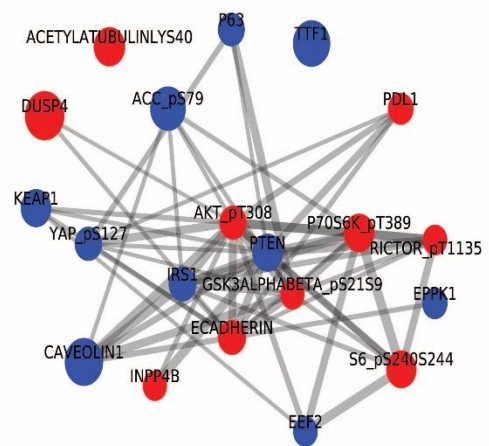
Figure S4

A

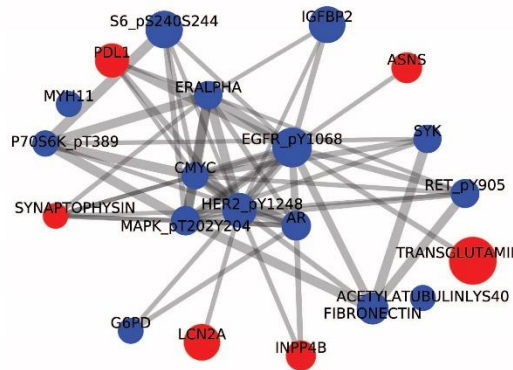




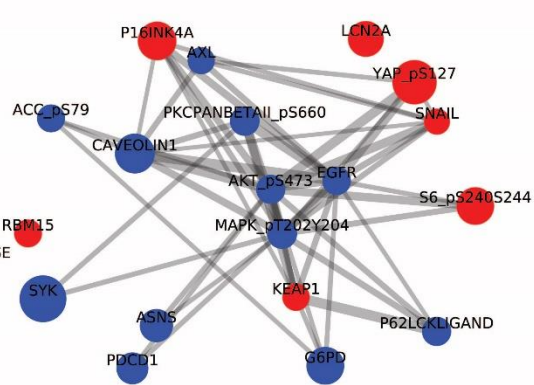
Unbalanced process 7



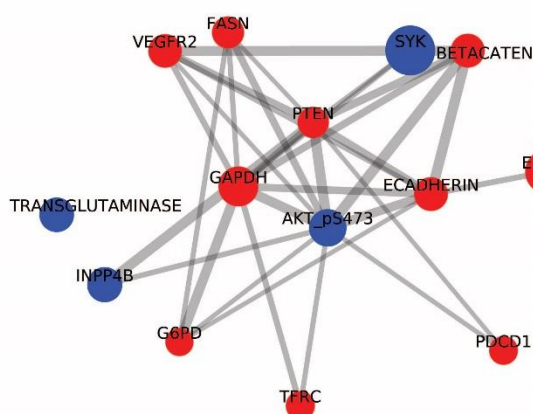
Unbalanced process 8



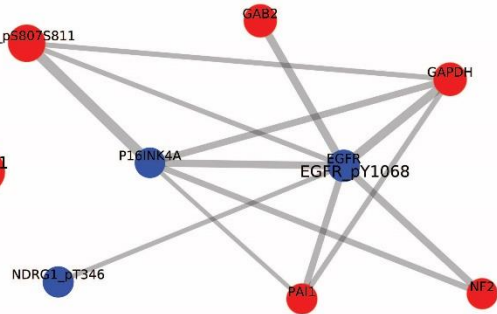
Unbalanced process 9



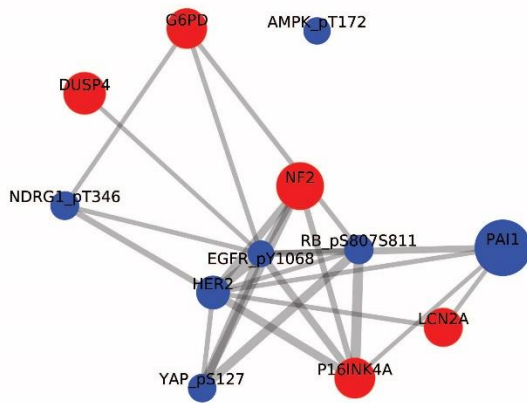
Unbalanced process 10



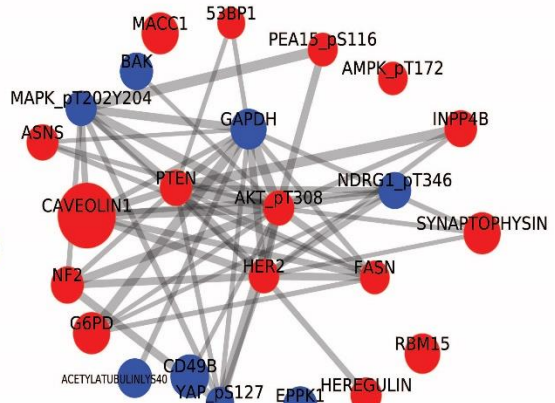
Unbalanced process 11



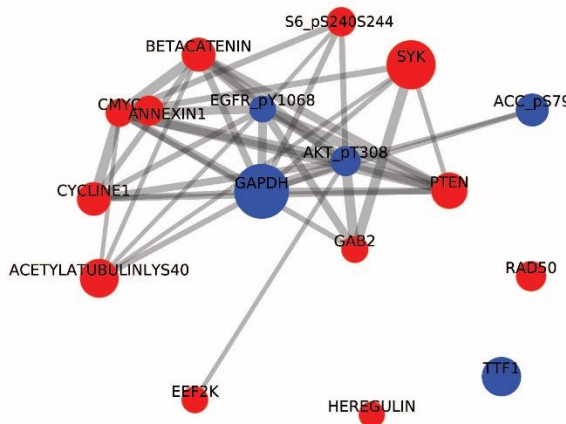
Unbalanced process 12



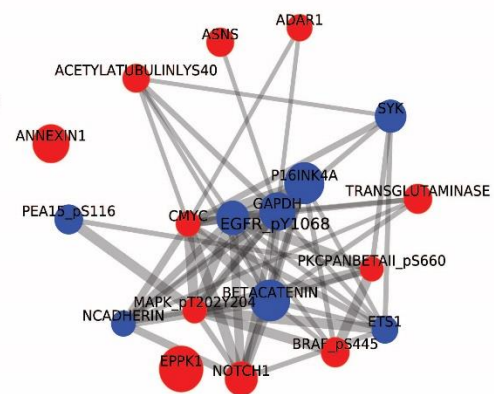
Unbalanced process 13



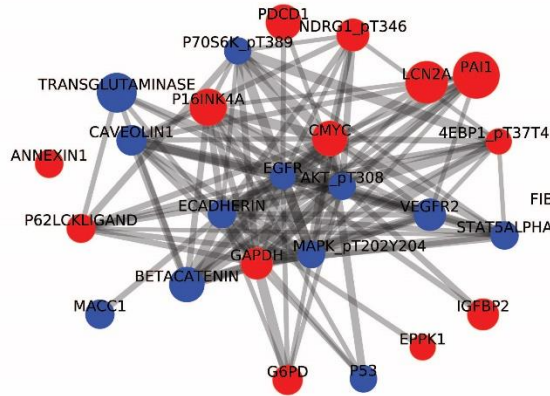
Unbalanced process 14



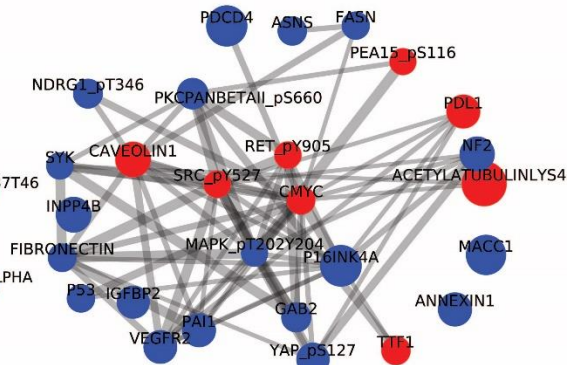
Unbalanced process 15



Unbalanced process 16



Unbalanced process 17



Unbalanced process 18

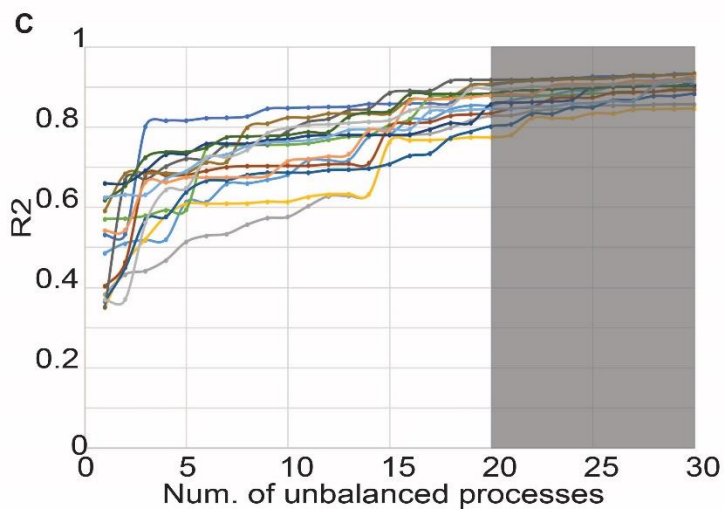
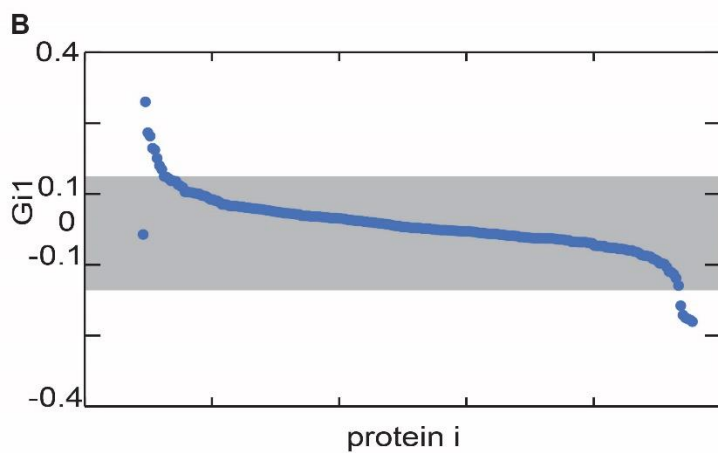
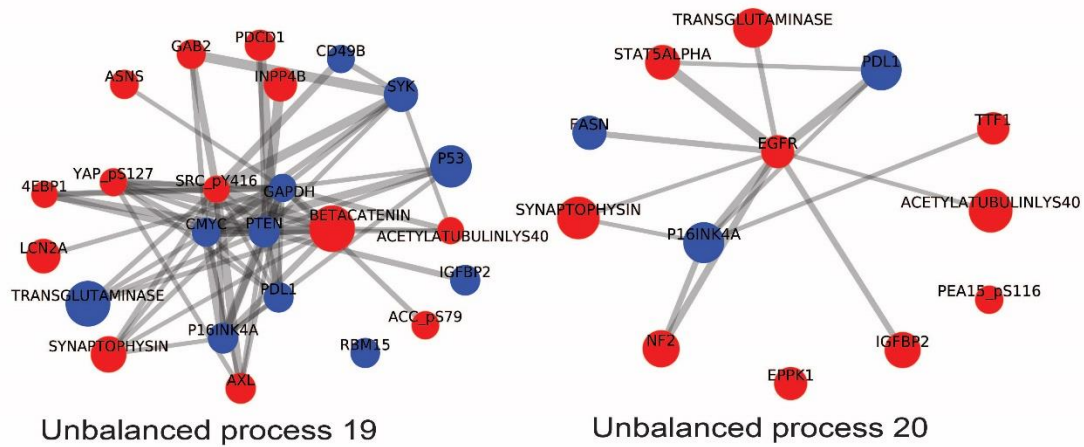


Figure S4. 20 unbalanced subnetworks, as identified by surprisal analysis, found to be active in 162 cancer cell lines. (A) 20 unbalanced processes characterizing 162 cancer cell lines. See Figure S4C demonstrating how the number of processes was determined. Proteins with negative $G_{i\alpha}$ values are labeled in blue and proteins with positive $G_{i\alpha}$ values in red, to distinguish between correlated and anti-correlated proteins. 20 unbalanced processes reproduce the experimental data. (B) Proteins must have a significant $G_{i\alpha}$ (which represent the degree of

participation of every protein i in the unbalanced process α , see Methods for more details) values to be included in the unbalanced process α . The proteins that take part in the different unbalanced processes were identified as follows: For every unbalanced process α , $G_{i\alpha}$ values were sorted according to their size, and only proteins with significant $G_{i\alpha}$ values were considered to participate in the unbalanced process α . This is exemplified for the process $\alpha = 1$. In the figure sorted values of G_{i1} are shown. The gray box represents threshold values. Proteins with $G_{i1} > 0.15$ or $G_{i1} < -0.15$ (which form the top and bottom "tails" of the distribution) were considered to participate the most in the unbalanced process $\alpha = 1$. These proteins were used to build a functional subnetwork using STRING database (showed in **A**). **(C)** R^2 values for 14 selected cell lines, are shown as an example. The R^2 was calculated by plotting the natural logarithm of the experimental data ($\ln X_i$) vs $\sum G_{i\alpha} \lambda_{\alpha}(k)$ for $\alpha = 1-30$. (see Figure legend S3 for more details). As we add more unbalanced processes, we expect to get higher correlation between the experimental data and the theoretical calculation ($\sum G_{i\alpha} \lambda_{\alpha}(k)$), reaching the highest level of correlation when the experimental data is reproduced by the theoretical fitting. The plot reaches a plateau after the 20th process. This indicates that after the 20th process the data includes mainly noise.

Figure S5

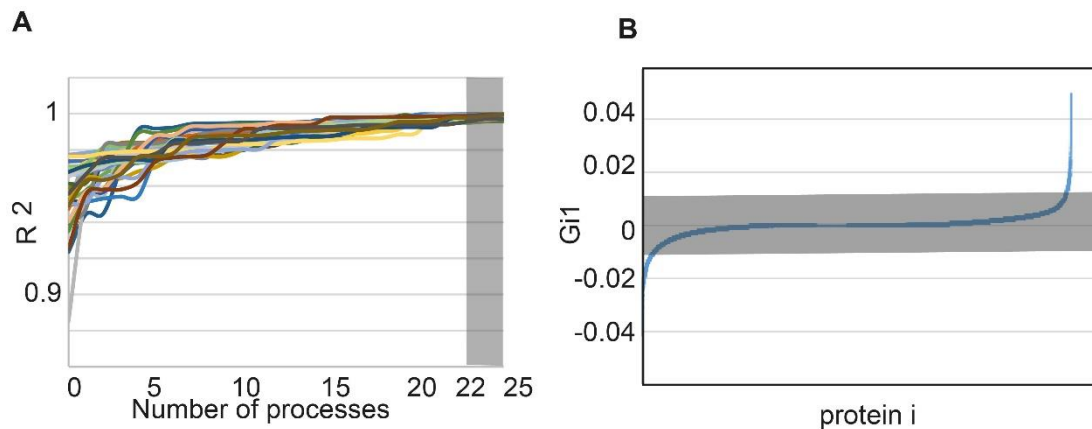


Figure S5. 22 unbalanced processes found to be active in 15 patient-derived HNSCC tissues treated with anti-EGFR monotherapy (A) R^2 values were calculated for all patients by plotting the natural logarithm of the experimental data against the sum of the gene expression level alterations due to unbalanced processes for different values of α . The figure shows that the plots for all patients reach a plateau after 22 processes, suggesting that the 22 unbalanced processes are significant, and the rest of the processes represent random noise in the samples. (B) The transcripts that take part in the different unbalanced processes were identified as follows: For every unbalanced process α , $G_{i\alpha}$ values were sorted according to their size, and only transcripts with significant $G_{i\alpha}$ values were considered to participate in the unbalanced process α . This is exemplified for the process $\alpha = 1$ in the figure. Shown are sorted values of G_{i1} , which represent the degree of participation of every transcript i in the unbalanced process $\alpha = 1$. The gray box represents threshold values. Transcripts with $G_{i1} > 0.015$ or $G_{i1} < -0.015$ (which are not contained in the gray box and form the top and bottom "tails" of the distribution) were considered to participate the most in the unbalanced process $\alpha = 1$. These transcripts were used to find a biological meaning of each unbalanced processes using David database.

References:

1. Remacle F, Kravchenko-Balasha N, Levitzki A, Levine RD. Information-theoretic analysis of phenotype changes in early stages of carcinogenesis. *Proc Natl Acad Sci U S A*. 2010;107(22):10324–9.
2. Vasudevan S, Flashner-Abramson E, Remacle F, Levine RD, Kravchenko-Balasha N. Personalized disease signatures through information-theoretic compaction of big cancer data. *Proc Natl Acad Sci U S A* [Internet]. 2018 Jul 24 [cited 2019 Aug 8];115(30):7694–9. Available from: <http://www.ncbi.nlm.nih.gov/pubmed/29976841>
3. Flashner-Abramson E, Vasudevan S, Adejumobi IA, Sonnenblick A, Kravchenko-Balasha N. Decoding cancer heterogeneity: Studying patient-specific signaling signatures towards personalized cancer therapy. *Theranostics*. 2019;9(18):5149–65.